Physics Letters A 376 (2012) 472–475

Contents lists available at SciVerse ScienceDirect

Physics Letters A

www.elsevier.com/locate/pla

Resonant invisibility with finite range interacting fermions

Jean-Pierre Nguenang [a,b], Sergej Flach [a], Ramaz Khomeriki [a,c,*]

[a] Max-Planck-Institut für Physik komplexer Systeme, Nöthnitzer Str. 38, 01187 Dresden, Germany
[b] Fundamental Physics Laboratory: Group of Nonlinear Physics and Complex Systems, Department of Physics, University of Douala, P.O. Box 24157, Douala, Cameroon
[c] Department of Physics, Tbilisi State University, 3 Chavchavadze, 0128 Tbilisi, Georgia

ARTICLE INFO

Article history:
Received 18 August 2011
Received in revised form 15 November 2011
Accepted 23 November 2011
Available online 28 November 2011
Communicated by A.R. Bishop

Keywords:
Cold atoms
Optical lattice
Hubbard model

ABSTRACT

We study the eigenstates of two opposite spin fermions on a one-dimensional lattice with finite range interaction. The eigenstates are projected onto the set of Fock eigenstates of the noninteracting case. We find antiresonances for symmetric eigenstates, which eliminate the interaction between two symmetric Fock states when satisfying a corresponding selection rule.

1. Introduction

Up to now a lot of interest in experiments on cold atoms has been focused on matter wave properties of the condensates which are described by the Hartree–Fock–Bogoliubov mean field model for weakly interacting quantum gases [1–5]. At the same time, the use of collision processes turns out to be a promising approach to implement quantum gate operations [6]. A standard method for the description of such systems is to map them to Hubbard like lattice models where atomic physics provides a whole toolbox to engineer various types of Hamiltonians for 1D, 2D, and 3D Bose and Fermi systems.

The interplay of interactions and discreteness leads to a set of interesting phenomena, including bound states, see e.g. [7–11] and [12,14,13]. In recent papers [15,16] we have studied properties of such bound states (also frequently coined quantum breathers) in various one-dimensional Hubbard like models by considering two bosons or two fermions (with opposite spins) on lattices. The fermionic case adds to the complexity with the spin as an additional degree of freedom. Consequently two fermions can form up to three different bound states, while two bosons form only one. In all these cases the interaction was assumed to be local, i.e. both particles interact only when occupying the same lattice site. In the present Letter we consider fermionic particles with a finite range of interaction, as a more realistic description of experimental situations, which may be directly applicable in quantum computing, where the controlled interaction can be used to create entanglement with high fidelity. We analyze two particle eigenfunctions and identify resonance conditions for which two particles do not scatter despite the presence of a nonzero interaction.

2. Model and spectrum

We consider one-dimensional periodic lattice with f sites described by an extended Hubbard model. The Hamiltonian is given by

$$\hat{H} = \hat{H}_0 + \hat{H}_U + \hat{H}_V, \tag{1}$$

$$\hat{H}_0 = -\sum_{j,\sigma} \hat{a}^+_{j,\sigma}(\hat{a}_{j-1,\sigma} + \hat{a}_{j+1,\sigma}), \tag{2}$$

$$\hat{H}_U = -U\sum_j \hat{n}_{j,\uparrow}\hat{n}_{j,\downarrow}, \quad \hat{n}_{j,\sigma} = \hat{a}^+_{j,\sigma}\hat{a}_{j,\sigma}, \tag{3}$$

$$\hat{H}_V = -V\sum_j \hat{n}_j\hat{n}_{j+1}, \quad \hat{n}_j = \hat{n}_{j,\uparrow} + \hat{n}_{j,\downarrow}. \tag{4}$$

Here $\hat{H}_0$ describes the nearest-neighbor hopping, $\sigma = \uparrow, \downarrow$ denotes the spin, $\hat{H}_U$ and $\hat{H}_V$ describe the onsite and intersite (between adjacent sites) interaction between the particles with strengths U and V, respectively; $a^+_{j,\sigma}$ and $a_{j,\sigma}$ are the fermionic creation and annihilation operators satisfying the anticommutation relations: $[\hat{a}_{j,\sigma}, \hat{a}^+_{l,\sigma'}] = \delta_{j,l}\delta_{\sigma,\sigma'}$, and $[\hat{a}_{j,\sigma}, \hat{a}_{l,\sigma'}] = [\hat{a}^+_{j,\sigma}, \hat{a}^+_{l,\sigma'}] = 0$. The sign of U and V is not specified. The Hamiltonian (1) commutes with the number operator $\hat{N} = \sum_j \hat{n}_j$ whose eigenvalues are $n = n_\uparrow + n_\downarrow$, which is the total number of fermions in the lattice. In

* Corresponding author at: Department of Physics, Tbilisi State University, 3 Chavchavadze, 0128 Tbilisi, Georgia. Tel./fax: +995 322915681.
E-mail addresses: nguenang@yahoo.com (J.-P. Nguenang), flach@pks.mpg.de (S. Flach), khomeriki@hotmail.com (R. Khomeriki).

0375-9601/$ – see front matter
doi:10.1016/j.physleta.2011.11.048

this work we focus on the simplest nontrivial case of $n = 2$, with $n_\uparrow = 1$ and $n_\downarrow = 1$.

To describe quantum states, we use a number state basis $|\Phi_n\rangle = |n_1; n_2 \cdots n_f\rangle$ [12], where $n_i = n_{i,\uparrow} + n_{i,\downarrow}$ represents the number of fermions at the i-th site of the lattice. The fermionic two particle states are generated from the vacuum $|O\rangle$ by successively creating a particle with spin down and spin up.

The Hamiltonian (1) commutes with the translational operator $\hat{T}$, which shifts all lattice indices by one. Its eigenvalues are $\tau = \exp(ik)$ with the Bloch wave number $k = \frac{2\pi\nu}{f}$, and $\nu = 0, 1, 2, \ldots, f-1$.

2.1. Single-fermion states

In this simplest case, only one fermion is in the lattice (either with spin up or down) ($n = 1$), and the state is represented by $|j\rangle = \hat{a}^+_{j,\sigma}|O\rangle$. The interaction terms ($\hat{H}_U$ and $\hat{H}_V$) have no contribution for a single particle. Thus the eigenstates of the Hamiltonian (1) are the eigenstates of $\hat{H}_0$ which are given by:

$$|\Psi_1\rangle = \frac{1}{\sqrt{f}} \sum_{s=1}^{f} \left(\frac{\hat{T}}{\tau}\right)^{s-1} |1\rangle. \tag{5}$$

The corresponding eigenenergies are

$$\varepsilon_k = -2\cos(k). \tag{6}$$

2.2. Two fermions

For the case of two opposite spin fermions ($n = 2$ with $n_\uparrow = 1$ and $n_\downarrow = 1$), each eigenstate is formed as a linear combination of number states with fixed n,

$$|\Psi_n\rangle = \sum_j c_j |\Phi_n^j\rangle. \tag{7}$$

For two particles, this involves $N_s = f^2$ basis states, $|\Phi_2^j\rangle$, which is the number of ways one can distribute two fermions with opposite spins over the f sites with possible double occupancy. Then we define the basis state with a given value of the wave number k as in Ref. [16] and a complete wave function is:

$$|\Psi_2^k\rangle = c_1|\Phi_1\rangle + \sum_{j=2}^{(f+1)/2} c_{j,+}|\Phi_{j,+}\rangle + \sum_{j=2}^{(f+1)/2} c_{j,-}|\Phi_j, -\rangle. \tag{8}$$

Here we consider the case of an odd number of lattice sites, the extension to even numbers is straightforward (see e.g. Ref. [12]). Any vector in the corresponding Hilbert space is spanned by the numbers $|c_1, c_{2,+}, c_{2,-}, c_{3,+}, c_{3,-}, \ldots\rangle$ and the vectors $|\Phi_1\rangle$, $|\Phi_{j,+}\rangle$ and $|\Phi_{j,-}\rangle$ in two fermion case are defined as follows:

$$|\Phi_1\rangle = \frac{1}{\sqrt{f}} \sum_{s=1}^{f} \left(\frac{\hat{T}}{\tau}\right)^{s-1} \hat{a}^+_{1,\uparrow}\hat{a}^+_{1,\downarrow}|O\rangle,$$

$$|\Phi_{j,+}\rangle = \frac{1}{\sqrt{f}} \sum_{s=1}^{f} \left(\frac{\hat{T}}{\tau}\right)^{s-1} \hat{a}^+_{j,\uparrow}\hat{a}^+_{1,\downarrow}|O\rangle,$$

$$|\Phi_{j,-}\rangle = \frac{1}{\sqrt{f}} \sum_{s=1}^{f} \left(\frac{\hat{T}}{\tau}\right)^{s-1} \hat{a}^+_{1,\uparrow}\hat{a}^+_{j,\downarrow}|O\rangle. \tag{9}$$

We diagonalize the Hamiltonian (1) in the framework of the basis defined in (8) and derive the eigenenergies for each given Bloch wave number k from $\hat{H}|\Psi_2^k\rangle = E|\Psi_2^k\rangle$. This leads to an $f \times f$ matrix whose elements $H_{i,j}$ $(i, j = 2, \ldots, (f+1)/2)$ are derived from

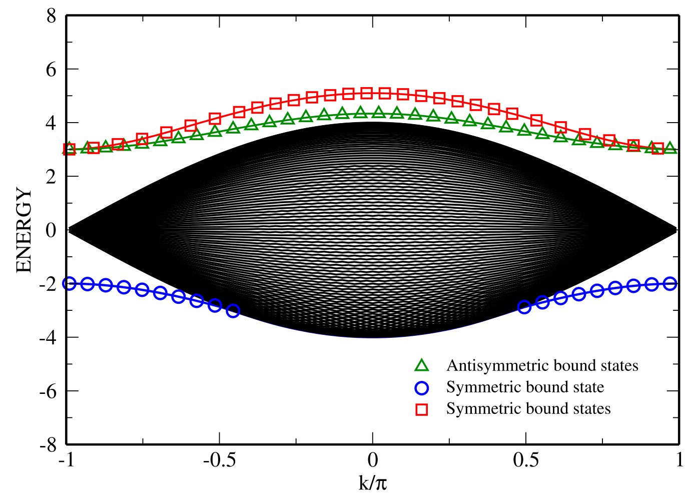

Fig. 1. Energy spectrum of two fermions of the extended Hubbard model with periodic boundary conditions for $U = 2$, $V = -3$ and $f = 101$. The lines follow from numerical diagonalization of the matrix (10) and symbols are the results of analytical computations for the bound states similar to the calculations in [16].

$$H_{i,1} = H^*_{1,i} = \langle\Phi_{i,\pm}|\hat{H}|\Phi_1\rangle, \qquad H_{i,j} = \langle\Phi_{i,\pm}|\hat{H}|\Phi_{j,\pm}\rangle. \tag{10}$$

We show in Fig. 1 the energy spectrum of the Hamiltonian matrix (10) obtained by numerical diagonalization for the case of opposite signs of interaction parameters $U = 2$ and $V = -3$ and the form of the spectrum is similar to the one in Ref. [16]. Besides a two particle continuum, three bound state bands are found. The eigenstates $|\Phi_{k_1,k_2}\rangle$ of the continuum correspond to two fermions independently moving along the lattice as with zero interaction, and are derived from (8). Their eigenenergies are given by:

$$E^0_{k,k_1} = -4\cos(k/2)\cdot\cos(k_1), \tag{11}$$

with k being the Bloch wave number and $k_1 = 2\pi\nu/(f-1)$, being the canonically conjugated momentum of the relative coordinate (distance) between both particles and $\nu = 0, \ldots, (f-1)/2$. Eq. (11) is the result of the sum of Bloch bands $E_\pm = -2\cos(\frac{k}{2} \pm k_1)$ of two asymptotically free particles [17].

3. Weight functions in normal mode space

We transform to the basis of the symmetric and antisymmetric states

$$|\Phi_{j,s}\rangle = \frac{|\Phi_{j,+}\rangle + |\Phi_{j,-}\rangle}{\sqrt{2}}, \qquad |\Phi_{j,a}\rangle = \frac{|\Phi_{j,+}\rangle - |\Phi_{j,-}\rangle}{\sqrt{2}} \tag{12}$$

where a and s refer to the antisymmetric and the symmetric states, respectively, $j = 2, \ldots, (f+1)/2$. Note that $|\Phi_1\rangle$ is also a symmetric state. In this basis the matrix (10) decomposes into two irreducible parts given by

$$H^s(i,j) = -\begin{pmatrix} U & q\sqrt{2} & & & & \\ q^*\sqrt{2} & V & q & & & \\ & q^* & 0 & q & & \\ & & \ddots & \ddots & \ddots & \\ & & & q^* & 0 & q \\ & & & & q^* & p \end{pmatrix}, \tag{13}$$

and

$$H^a(i,j) = -\begin{pmatrix} V & q & & & & \\ q^* & 0 & q & & & \\ & q^* & 0 & q & & \\ & & \ddots & \ddots & \ddots & \\ & & & q^* & 0 & q \\ & & & & q^* & -p \end{pmatrix}, \tag{14}$$

with $q = 1 + \tau$ and $p = \tau^{-(f+1)/2} + \tau^{-(f-1)/2}$. The rank of the symmetric matrix is $(f+1)/2$ and the rank of the antisymmetric matrix is $(f-1)/2$.

Our strategy is to compute an eigenstate for the interacting case, and expand it in the basis of the eigenstates of the noninteracting case. For this purpose we fix the Bloch momentum k, and choose a seed eigenstate $|\Psi^0_{\tilde{k}_1}\rangle$ of the unperturbed case with seed mode number $\tilde{k}$. Upon switching on the interaction it becomes a new eigenstate $|\Psi_{\tilde{k}_1}\rangle$, which will have overlap with several eigenstates of the unperturbed case. We expand the eigenfunction of the perturbed system using first order perturbation approximation:

$$|\Psi_{\tilde{k}_1}\rangle = |\Psi^0_{\tilde{k}_1}\rangle + \epsilon \sum_{k'_1 \neq \tilde{k}_1} \frac{\langle \Psi^0_{k'_1}|\hat{H}_U + \hat{H}_V|\Psi^0_{\tilde{k}_1}\rangle}{E^0_{\tilde{k}_1} - E^0_{k'_1}} |\Psi^0_{k'_1}\rangle \tag{15}$$

and define the weight function as the square of the projection of this eigenstate on the unperturbed eigenfunction space:

$$C^s(k_1;\tilde{k}_1) = \left|\langle \Psi^0_{k_1}|\Psi_{\tilde{k}_1}\rangle\right|^2. \tag{16}$$

Then from expansion (15) it follows that the off-diagonal terms in the $(k_1 \neq \tilde{k}_1)$ weight function at first order are given by:

$$C^s(k_1;\tilde{k}_1) = \frac{(2U|q|^2 + V E^0_{k_1} E^0_{\tilde{k}_1})^2 |(\langle \Psi^0_{k_1}|)_1 (|\Psi^0_{\tilde{k}_1}\rangle)_1|^2}{4|q|^4 (E^0_{\tilde{k}_1} - E^0_{k_1})^2}, \tag{17}$$

with $|q|^2 = 2 + 2\cos(k)$. Here $E^0_{k_1}$ and $E^0_{\tilde{k}_1}$ are the eigenenergies of the unperturbed system given by Eq. (11), and $(|\Psi^0_{\tilde{k}_1}\rangle)_1$ defines the first component of the eigenvector $|\Psi^0_{\tilde{k}_1}\rangle$.

3.1. Symmetric states

First we consider the case of small interaction constants and as expected we find localization in normal mode space. For instance, in the case of dominant onsite interaction constant $U = 1$ and $V = 0.1$, quite similar results to those obtained in Ref. [15] characterizing quantum q-breathers properties are derived and the result of the perturbation formula (17) matches pretty well with those of the diagonalization procedure. But if now we take interaction constants U, V with comparable values (but again in perturbative limit) one will unavoidable deal with additional antiresonance structure presented in Fig. 2, where the weight function vanishes exactly. The appearance of these structures follows from the analytical formula (17). Indeed, in perturbative limit of interaction constants one can find such a seed $\tilde{k}_1$ and probe k_1 wave numbers that the weight function becomes exactly zero. We find the following condition for zero weight:

$$\frac{U}{V} = -2\cos(k_1)\cos(\tilde{k}_1). \tag{18}$$

It also follows from Eq. (18) that there is a critical wave number given by

$$k^c_1 = \arccos\left(-\frac{U}{2V}\right). \tag{19}$$

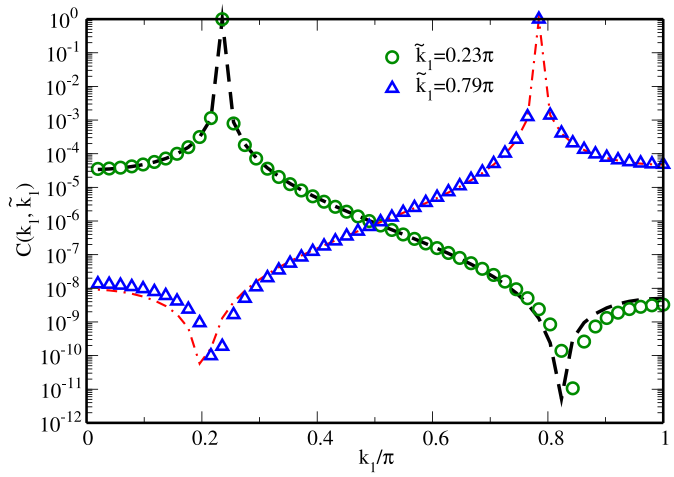

Fig. 2. Weight function for two seed mode numbers $\tilde{k}_1 = 0.23\pi$ and $\tilde{k}_1 = 0.79\pi$, with the onsite and intersite interaction parameters $U = 0.1$ and $V = 0.08$. Here $k = 0.5\pi$ and $f = 101$. Dashed lines are the results using formula (17).

An antiresonance appears only if the following inequalities are satisfied: $\pi - k^c_1 < \tilde{k}_1 < k^c_1$ (here for simplicity we assume both interaction constants positive). As it is seen from Fig. 2 the perturbative limit (17) works well even in case of presence of an antiresonance. Eq. (18) further tells that an antiresonance will be observed even for $U = 0$. In this case the seed wave number $\tilde{k}_1 = \pi/2$ is not modified by interaction V. On the other hand if $V = 0$ the antiresonances are not observable.

For larger values of interaction constants the perturbative predictions will get significant corrections. To show this we plot three-dimensional graphs of weight function versus seed $\tilde{k}_1$ and probe k_1 wave numbers for various values of interaction constants in Fig. 3. As seen for small values of interaction constants the track of the antiresonances keeps the symmetry in the seed-probe mode number space traces predicted by perturbation theory. However for large interaction constants this symmetry is lost.

3.2. Antisymmetric states

The structure of the antisymmetric matrix (14) suggests that the weight function for antisymmetric states can be computed as:

$$C^a(k_1;\tilde{k}_1) = \frac{V^2 |(\langle \Psi^0_{k_1}|)_1 (|\Psi^0_{\tilde{k}_1}\rangle)_1|^2}{(E^0_{\tilde{k}_1} - E^0_{k_1})^2}, \tag{20}$$

and according to this formula the weight function does not develop antiresonances. This has been confirmed by numerical diagonalization.

4. Discussions

Let us discuss the meaning of the observed antiresonances. Two particles, when travelling along the lattice, will meet, interact, and scatter. If prepared in an initial symmetric noninteracting seed state, the particles will scatter into all other available noninteracting symmetric states – except for one special case: when the weight function defined by (16) vanishes. This cancellation happens because the scattering can go either via the onsite interaction U or via the intersite interaction V. A corresponding destructive interference makes the amplitude in this particular scattering state exactly zero. Antisymmetric states have strict zero occupation on the same site, and therefore only one scattering path (using V) is left. Consequently they do not show antiresonances. But they will,

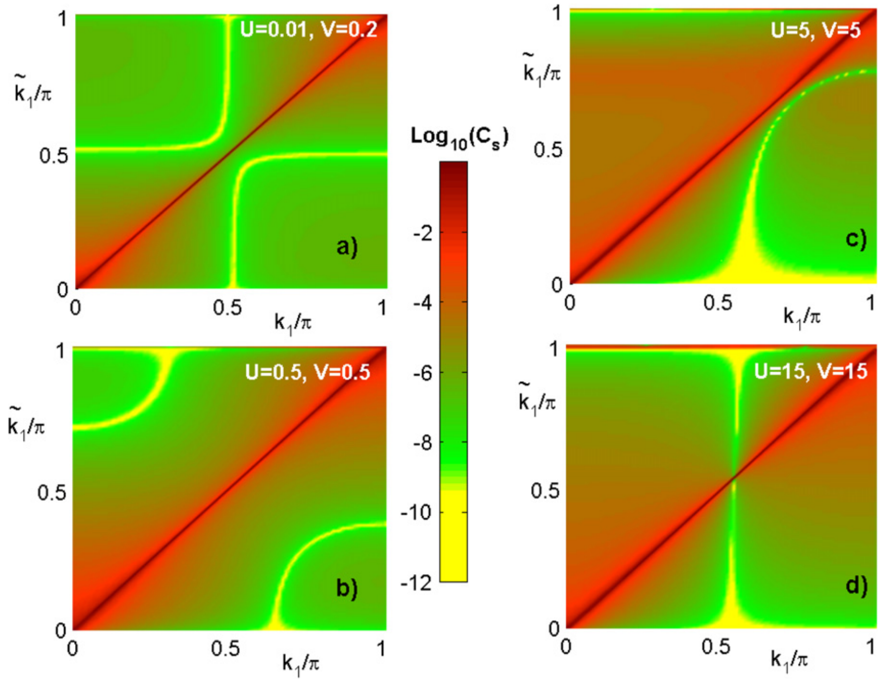

Fig. 3. Three-dimensional plots of the weight function for symmetric states for a fixed value of the Bloch wave number $k = 0.12\pi$ and different interaction constants U and V. The lattice size is the same $f = 101$ as in the previous plots. Red peak structure is a signature of quantum q-breathers and yellow antipeak traces displays the invisibility places. (For interpretation of colors in this figure, the reader is referred to the web version of this Letter.)

if we add even more distant (e.g. next-to-nearest-neighbor) interactions and/or consider more realistic potentials. Here we have chosen the simple interaction scheme in order to show the invisibility effect which might be useful for quantum computing purposes.

Acknowledgements

J.-P. Nguenang and R. Khomeriki acknowledge the warm hospitality of the Max Planck Institute for the Physics of Complex Systems in Dresden.

References

[1] K. Southwell, Nature 416 (2002) 205.
[2] F. Dalfogo, S. Giorgini, L. Pitaevskii, S. Stringari, Rev. Mod. Phys. 71 (1999) 463.
[3] A. Leggett, Rev. Mod. Phys. 73 (2001) 307.
[4] L. Pitaevskii, S. Stringari, Bose–Einstein Condensation, Oxford University Press, Oxford, 2003.
[5] C. Pethick, H. Smith, Bose–Einstein Condensation in Dilute Gases, Cambridge University Press, Cambridge, 2001.
[6] O. Mendel, M. Greiner, A. Widera, T. Rom, T.W. Hansch, I. Bloch, Nature 425 (2003) 937.
[7] V. Fleurov, Chaos 13 (2003) 676.
[8] A.C. Scott, Nonlinear Science, Oxford University Press, Oxford, 1999.
[9] R.A. Pinto, S. Flach, Phys. Rev. A 73 (2006) 022717.
[10] R.A. Pinto, S. Flach, Europhys. Lett. 79 (2007) 66002.
[11] R.A. Pinto, S. Flach, Phys. Rev. B 77 (2008) 024308.
[12] A.C. Scott, J.C. Eilbeck, H. Gilhøj, Physica D 78 (1994) 194.
[13] V. Pouthier, Phys. Rev. E 68 (2003) 021909.
[14] J. Dorignac, J.C. Eilbeck, M. Salerno, A.C. Scott, Phys. Rev. Lett. 93 (2004) 025504.
[15] J.P. Nguenang, R.A. Pinto, S. Flach, Phys. Rev. B 75 (2007) 214303;
R.A. Pinto, J.P. Nguenang, S. Flach, Physica D 238 (2009) 581.
[16] J.P. Nguenang, S. Flach, Phys. Rev. A 80 (2009) 015601.
[17] M. Valiente, D. Petrosyan, J. Phys. B: At. Mol. Opt. Phys. 41 (2008) 161002.